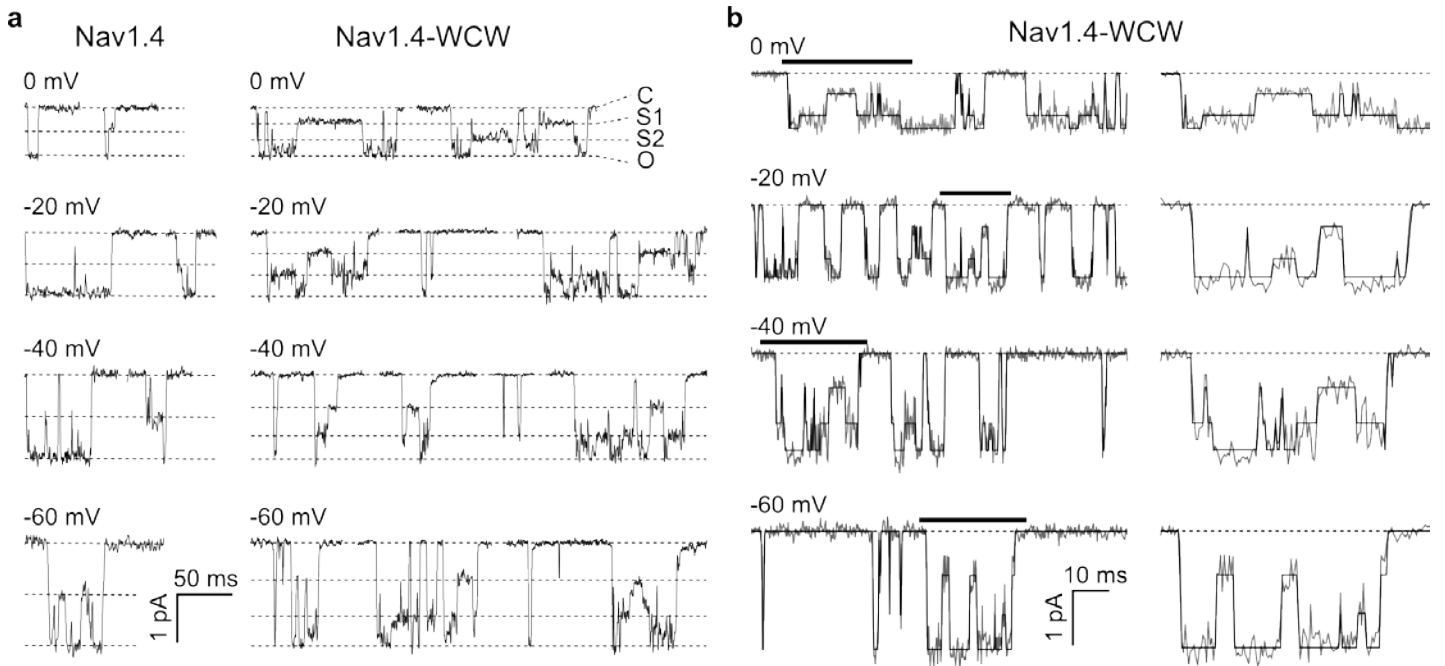
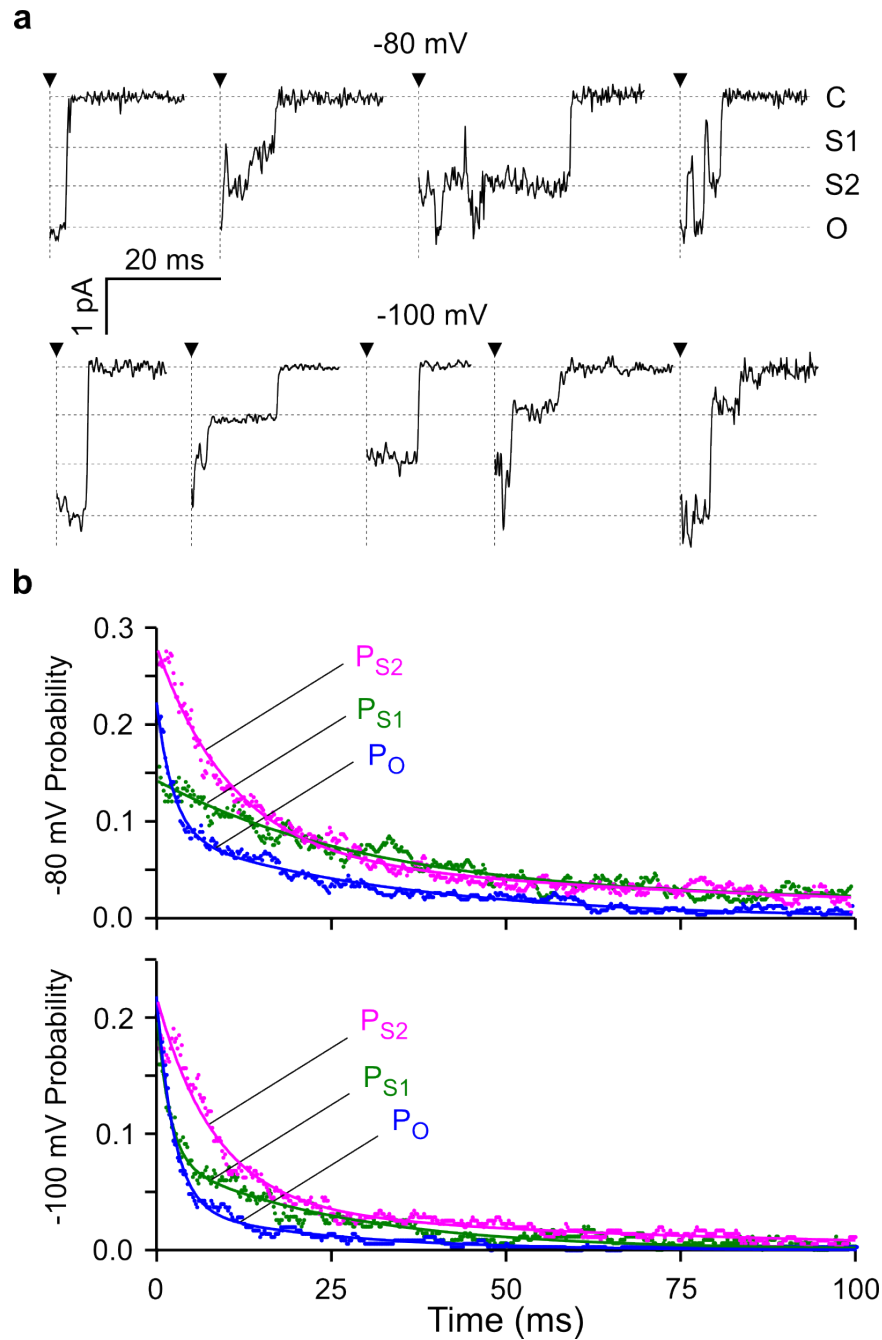


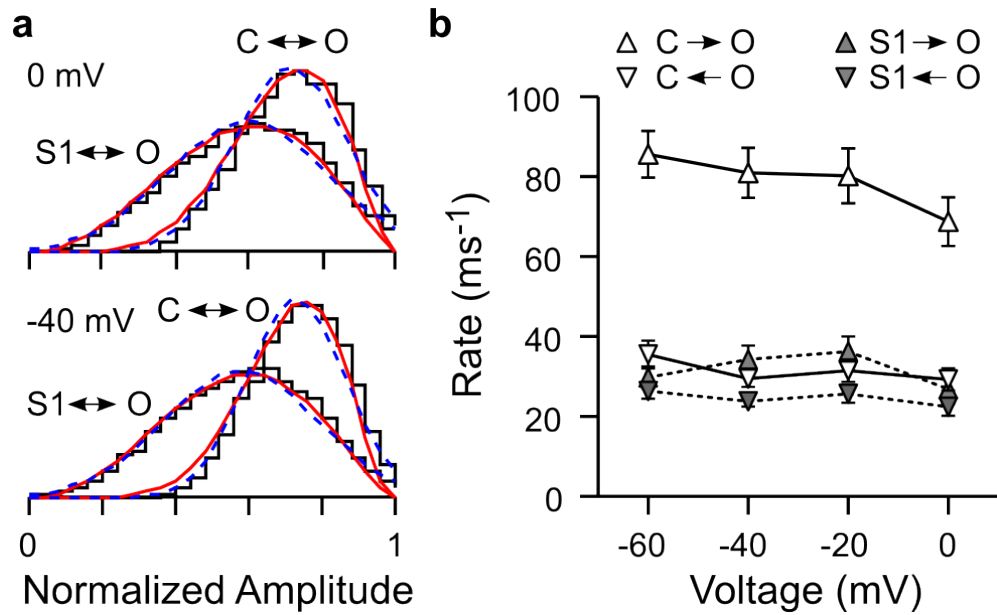
Supplementary Figure S1. Kinetics of macroscopic current rise in wild type and Nav1.4-WCW channels. (a) The time course of current activation from the time at which the current was equal to half of the peak response up until the peak was fit to the equation $I_{\text{peak}} (1 - \exp(-(t - t_0) / \tau_a))$, where I_{peak} is the peak current, t is time, t_0 is the time of current onset which was allowed to lag the onset of the voltage step, and τ_a is the time constant of current activation. Example trace is for Nav1.4-WCW. (b, c) Voltage dependence of activation from fits as described in a (mean \pm s.e.m.).



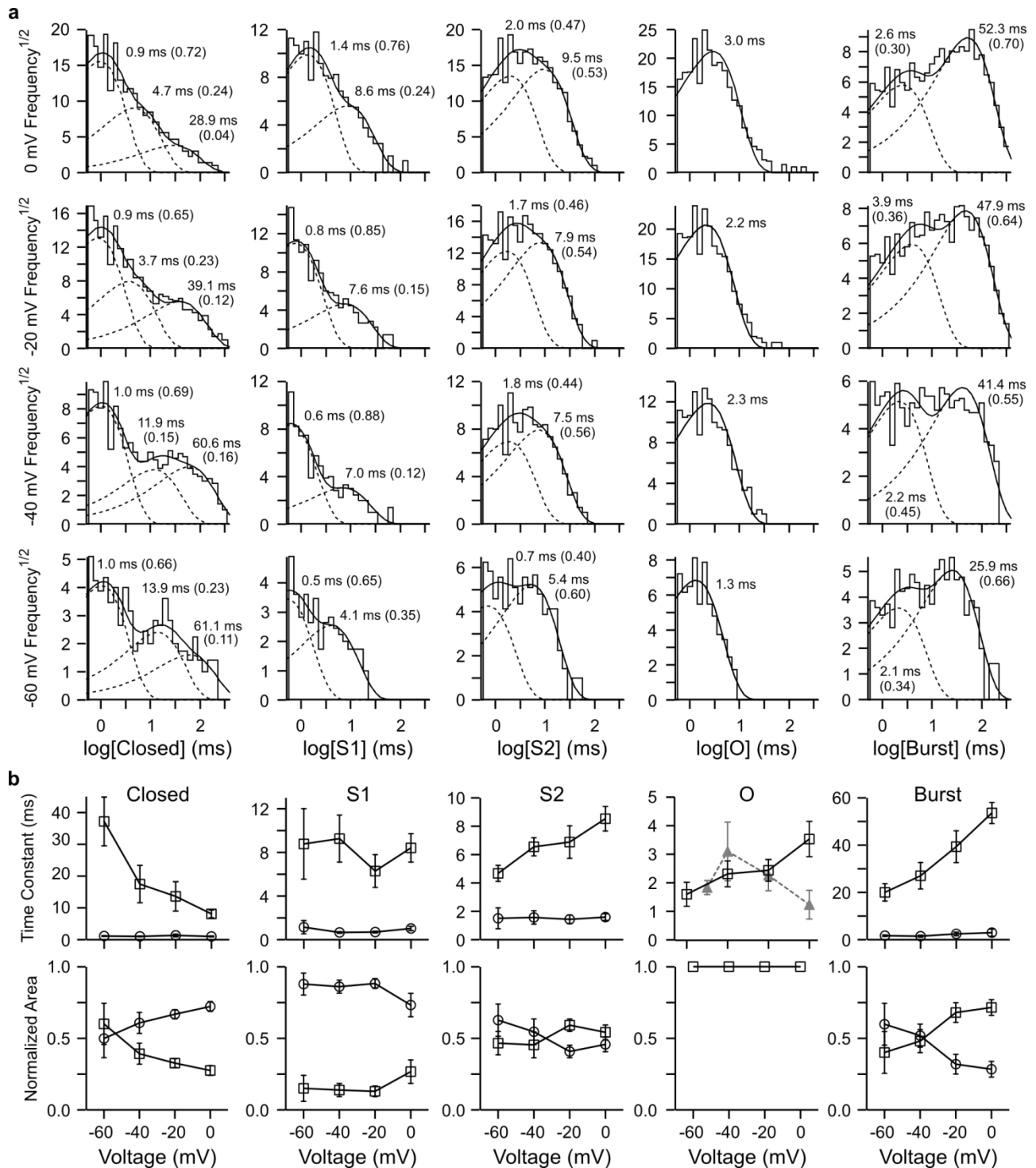
Supplementary Figure S2. Subconductances in Nav1.4 and Nav1.4-WCW channels. (a) Examples of subconductance events for Nav1.4 (left) and Nav1.4-WCW (right) channels during activation from -60 to 0 mV (dashed lines indicate observed conductance levels including the closed channel baseline, openings are downward). Responses were filtered at 1 kHz for display. (b) Example idealizations (solid black) of single Nav1.4-WCW channel activation records (gray, filtered at 2 kHz) including two subconductance levels obtained using the segmental k-means method in QuB³¹ (see methods in main text). The portion of each trace indicated by a black bar is shown on an expanded timescale to the right.



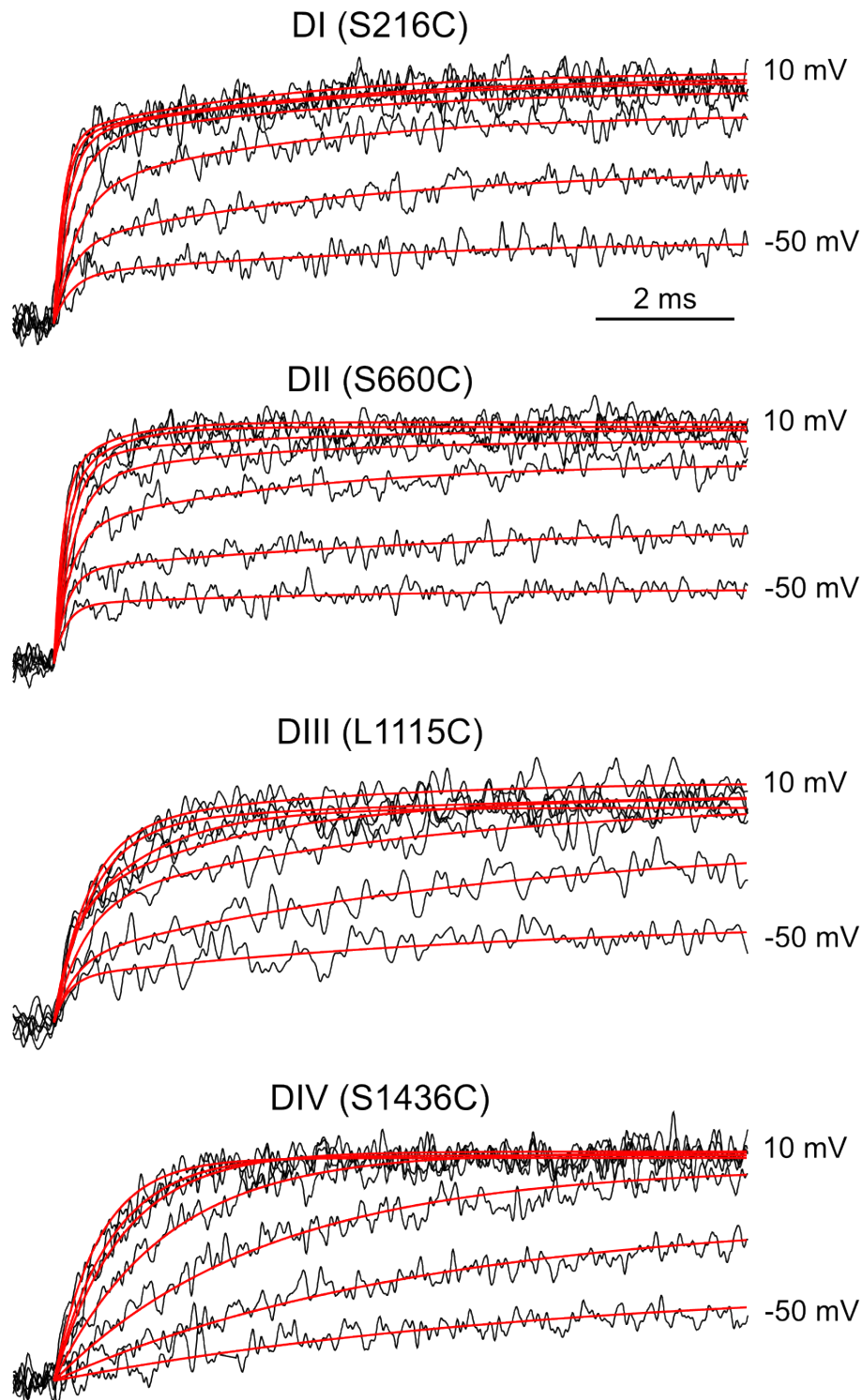
Supplementary Figure S3. Nav1.4-WCW single channel deactivation. (a) Deactivation of single Nav1.4-WCW channels at -80 and -100 mV following a 40 ms depolarizing pulse to 50 mV from a holding potential of -120 mV. Black arrows and vertical dashed lines indicate the onset of deactivation at the end of the activating pulse. Horizontal dashed lines illustrate the observed conductance levels. (b) The time dependent probability in each conductance level obtained from the idealized records (dots). Smooth lines are fits to the equation $\sum_i A_i \exp(-t/\tau_i)$, where A_i and τ_i are the amplitudes and time constants of an exponential decay (S1 at -80 mV: $\tau_1 = 32.4$ ms, $A_1 = 0.14$; S2 at -80 mV: $\tau_1 = 10.7$ ms, $\tau_2 = 89.5$ ms, $A_1 = 0.21$, $A_2 = 0.07$; O at -80 mV: $\tau_1 = 2.4$ ms, $\tau_2 = 34.0$ ms, $A_1 = 0.14$, $A_2 = 0.09$; S1 at -100 mV: $\tau_1 = 1.7$ ms, $\tau_2 = 25.4$ ms, $A_1 = 0.12$, $A_2 = 0.08$; S2 at -100 mV: $\tau_1 = 8.3$ ms, $\tau_2 = 66.2$ ms, $A_1 = 0.18$, $A_2 = 0.04$; O at -100 mV: $\tau_1 = 2.4$ ms, $\tau_2 = 22.5$ ms, $A_1 = 0.19$, $A_2 = 0.04$).



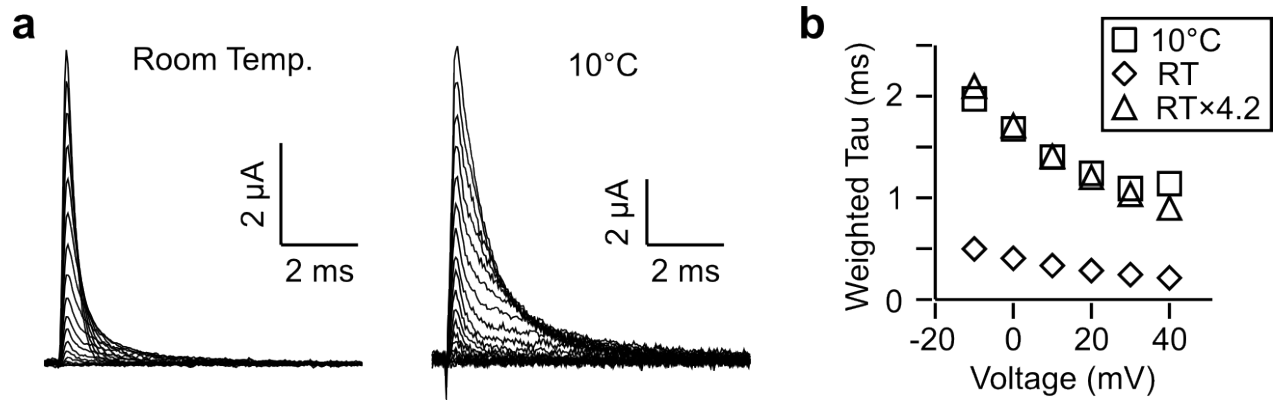
Supplementary Figure S4. Flicker analysis of a Nav1.4-WCW subconductance level. (a) Nav1.4-WCW amplitude histograms from channel activity during events at the S2 subconductance level after normalizing to the range [C = 0, O = 1] (C ↔ O) or [S1 = 0, O = 1] (S1 ↔ O). The first and last data points in each event were discarded to remove artifacts introduced by the filtering of the event onset and offset transitions. Histograms were fit with a beta distribution (solid red) or a Gaussian (dashed blue). (b) Mean ± s.e.m. across patches for the potential rate of flicker between either C and O or S1 and O estimated from beta distribution fits to the amplitude histograms as described by Yellen³³.



Supplementary Figure S5. Voltage dependence of apparent dwell times in individual conductance levels during Nav1.4-WCW activation. (a) Dwell time distributions from idealized records for each conductance level excluding events shorter than 0.5 ms. Smooth curves are the maximum log likelihood fit for 1-3 exponential components (dashed lines are individual components and the solid line is their sum)³⁶. Time constants (and relative areas) for each component are shown. (b) Mean \pm s.e.m. from maximal likelihood fits to dwell time distributions for individual patches as shown in a. The time constant (and relative area) of the fast (circles) and slow* (squares) components are shown. *For the closed times the slow component is the sum of the two longest closed times weighted by their individual areas (and the sum of their areas). Open times from single exponential maximum log likelihood fits to Nav1.4 are shown as gray triangles for comparison.



Supplementary Figure S6. Kinetics of fluorescent responses from fluorophores attached to introduced cysteines in each individual voltage sensor track entry into conductance levels O and S2. Fluorescent responses from site specific fluorophores in each voltage sensor as previously described by Chanda and Bezanilla¹⁸ during voltage steps from -50 to 10 mV from a holding potential of -130 mV. Kinetics were determined from biexponential fits (red) to fluorescence signals (black), with the exception of domain IV, which was fit with a monoexponential.



Supplementary Figure S7. ON gating currents from Nav1.4 after pore block with TTX at two different temperatures. (a) ON gating currents recorded from cut-open oocytes in a custom peltier driven temperature controlled chamber. Protocol consisted of depolarizing voltage steps from a holding potential of -130 mV up to 40 mV in 10 mV steps. (b) Weighted time constant from bi-exponential fits to the decay of ON gating currents elicited at depolarized potentials. The time constants at room temperature superimposed on those obtained at 10 °C upon scaling by a factor of 4.2.

Supplementary Table S1. Nav1.4-WCW dwell time distributions for each conductance level.

	Voltage (mV)	τ_1 (ms)	τ_2 (ms)	A_1
Closed*	0	1.0 ± 0.1	8.1 ± 1.2	0.72 ± 0.03
	-20	1.3 ± 0.4	13.6 ± 4.6	0.67 ± 0.03
	-40	1.0 ± 0.1	17.5 ± 5.9	0.61 ± 0.07
	-60	1.1 ± 0.1	37.2 ± 7.7	0.50 ± 0.13
Burst	0	3.0 ± 1.5	53.6 ± 4.5	0.28 ± 0.06
	-20	2.5 ± 0.7	39.3 ± 6.7	0.32 ± 0.07
	-40	1.5 ± 0.4	27.1 ± 5.6	0.52 ± 0.08
	-60	1.7 ± 0.3	20.0 ± 3.7	0.60 ± 0.15
S1	0	1.0 ± 0.2	8.4 ± 1.3	0.73 ± 0.08
	-20	0.7 ± 0.1	6.3 ± 1.5	0.88 ± 0.03
	-40	0.7 ± 0.1	9.3 ± 2.2	0.86 ± 0.05
	-60	1.1 ± 0.6	8.8 ± 3.2	0.88 ± 0.08
S2	0	1.6 ± 0.2	8.5 ± 0.9	0.46 ± 0.05
	-20	1.4 ± 0.3	6.9 ± 1.1	0.41 ± 0.04
	-40	1.6 ± 0.5	6.5 ± 0.6	0.55 ± 0.09
	-60	1.5 ± 0.7	4.7 ± 0.6	0.63 ± 0.11
Open	0	3.5 ± 0.6	n/a	1.0
	-20	2.4 ± 0.4	n/a	1.0
	-40	2.3 ± 0.5	n/a	1.0
	-60	1.6 ± 0.4	n/a	1.0
Open (Nav1.4)	0	1.2 ± 0.5	n/a	1.0
	-20	2.3 ± 0.5	n/a	1.0
	-40	3.1 ± 1.0	n/a	1.0
	-50	1.8 ± 0.2	n/a	1.0

Time constants τ_i (and normalized areas A_i) from maximum log likelihood exponential fits to dwell time distributions³ in individual conductance levels during Nav1.4-WCW activation (mean ± s.e.m.; 9 patches). * The closed channel slow time constants (τ_2) are the weighted average of the two slowest components from a three component fit to the closed dwell time distributions.

Supplementary Table S2. Kinetics of individual conductance levels.

	Voltage (mV)	A₁	τ₁ (ms)	C
P₀	0	0.26	1.9	n/a
	-20	0.17	2.7	n/a
	-40	0.07	6.7	n/a
	-60	0.05	27.5	n/a
P_{S2}	0	0.32	9.4	n/a
	-20	0.25	12.4	n/a
	-40	0.09	16.1	n/a
	-60	0.07	53.8	n/a
P_{S1}	0	0.08	11.2	n/a
	-20	0.07	8.9	n/a
	-40	0.03	15.5	n/a
	-60	0.02	41.5	n/a
CP₀	0	0.22	3.3	0.19
	-20	0.25	3.8	0.18
	-40	0.19	2.2	0.1
	-60	0.16	4.7	0.08
CP_{S2}	0	0.17	5.0	0.33
	-20	0.1	3.2	0.28
	-40	0.03	2.0	0.18
	-60	0.04	10.7	0.1
CP_{S1}	0	0.02	35.5	0.08
	-20	n/a*	n/a*	0.07
	-40	0.01	11.4	0.05
	-50	0.03	16.1	0.03

Fast time constants τ_1 (and amplitudes A_1) from mono- or bi-exponential fits to the kinetics of the time dependent probability in each individual conductance level (P_x was fit with the equation $\sum_i A_i [1 - \exp(-t/\tau_i)]$) and the conditional probability after first opening (CP_x was fit with the equation $\sum_i A_i \exp(-t/\tau_i) + C$) (see main text Fig. 5). * Could not be distinguished from a horizontal line.